

## The Study of Using External Fluid Loading on a Vibrating Rectangular Plate for Suspended Sediment Concentration in Water

Y.C. Liu<sup>1,2</sup>, Y.H. Hsu<sup>1,3</sup>, Y.S. Hsu<sup>1,4</sup> and J.H. Huang<sup>1,5</sup>

**Abstract:** This paper presents the result of a theoretical study on a new fluid density measuring concept which uses the effect of external fluid loading on a vibrating thin plate. The underlying physical principle of this concept is that the resonance frequencies of an immersed vibrating plate change with the surface impedance changes caused by the mass density variations of the external fluid. In this paper, the analytical solutions of resonance frequencies with specific gravity are demonstrated by a COMSOL the finite element simulation. The theoretical analysis presented in this paper shows that the resonance frequencies of an immersed vibrating thin plate affect significantly with surrounding fluid loading, which is loaded as an extra added mass. The resonance frequencies shifted to lower frequencies when the fluid specific gravity increased. For the resonance frequency ratio applied to the specific gravity estimation of onsite measurement, the increases in this coefficient are directly proportional to the increase with the specific gravity. In addition, size effect on the thin plate is also presented. The results show that the thickness of the thin plate is the most important factor for this resonance frequency ratio. Finally, the preliminary experiment of the thin plate immersed in the various fluid loading is also accomplished. The comparison shows that the experimental results agree reasonably well with the finite element simulation. Based on these results of the theoretical analysis and the experiment in this paper, using the loading by the external fluid on the vibrating thin plate is feasible.

**Keywords:** Vibrating Plate, Fluid Loading, Suspended Sediment Concentration, Resonance Frequency.

---

<sup>1</sup> Feng Chia University, No. 100 Wenhwa Rd., Seatwen, Taichung, Taiwan 40724, R.O.C..

<sup>2</sup> Department of Mechanical and Computer-Aided Engineering; yucliu@fcu.edu.tw.

<sup>3</sup> Research and Development Division Research Center for Science and Technology Across the Taiwan Strait; yuhsiung@mail2000.com.tw.

<sup>4</sup> Department of Water Resources Engineering and Conservation; yhsu @fcu.edu.tw

<sup>5</sup> Acoustic Graduate Program; jhhuang@fcu.edu.tw

## **1 Introduction**

Measurements of fluid density are required in various industries and scientific fields; for examples: industrial, mechanical, chemical, agricultural, and mining engineering. In hydrological and water resources engineering, measuring the density of turbid water may offer a great potential for an indirect method for determining the onsite suspended sediment concentration (SSC) in water bodies (Yin-Sung Hsu and Cai, Jun-Feng, 2010). This is the so-called densimetric technique for SSC, which is one of the more recently developed indirect methods intended to remedy the many drawbacks of the convectional direct method. The advantage of this method is that it offers automated real-time onsite measurements plus instant digital data capability.

Density measurements may be categorized as the traditional and modern methods. The former includes the density bottle and the hydrometer methods. The density bottle method offers good measurement precision and has a wide range of applications, but its measurement operation is cumbersome and complicated. The hydrometer method is easier to operate but offers only to some applications. The common drawbacks of the traditional methods are that both the measurement operation and reading are performed manually and are more susceptible to error. The modern methods include the float, ultrasonic, nuclear, electromagnetic, desimetric and vibration methods. Although these modern methods can only provide indirect measurements but they offer the advantageous automated and real-time capability. However, these methods are often subjected to severe environmental constrains.

Presently, all of the vibration methods utilize liquid-filled vibrating tubes which are excited to vibrate by electromagnetic actuations. The resonance frequencies of the tube vary with the densities of the fluid that flows inside the tube. In 1986, Hinghofer-Szalkay H. pioneered that the mechanical oscillator technique (MOT) for fluid density measurement had used this method by Leopold (1969). Due to their versatility, reliable, high precision, and ease to use, the vibrating tube type densimeters have become more popular. The United States Geological Survey (USGS) had developed several types of vibration densimeters. The types may be categorized according to the geometry of the tube, e.g., single-tube, double-tube, and U-tube (Guy H. and Norman V., 1970), etc. Among them the U-tube type is the most frequently used. The theoretical basis for the vibrating tube densimeters is that the square of the resonance frequency of a bending vibration mode is proportional to the ratio between the tube stiffness and the total mass of the tube, which includes the mass of the tube material and that of the fluid inside. Since the stiffness and the tube material mass are fixed constants, the resonance frequency will vary with the mass of the fluid contained inside the tube. Sultan G. and Hemp J. (1989) had theoretically derived and experimentally verified the relationship between res-

onance frequency and fluid mass. Based on this study, he developed the theoretical foundation for the Coriolis mass flowmeter. In 1999, Kalotay Paul obtained the fluid mass density from the measured resonance frequency of a liquid filled tube. In addition, the kinematic coefficients of viscosity were also estimated according to the inlet-outlet pressure differences. In order to reduce the noise interference and to improve measurement accuracy, Henry M. (2000) used an electronic data acquisition system to obtain the resonance frequencies via discrete Fourier transform of the acquired data.

The currently available vibrating tube densimeters are all liquid-filled type (usually a U-shaped tube). The shortcoming of this internal flow based measuring system is that it must be forced to overcome the tube wall resistance, the physical properties of the fluid sample inside the tube may be somewhat altered and no longer completely representing the properties of the fluid to be measured. When the fluid is transported as a slow two-phase flow containing heavy particles, deposits may build up on the tube wall. Eventually, the tube may get clogged due to the restricted area inside the tube. Under such circumstance, the fluid density inside the tube will be no longer representing that intended to be measured.

In order to remedy the shortcomings of the internal flow based measuring system, Hsu, Hwang and Huang. (2008) proposed the use of external fluid loading on a vibrating tube for measuring the density of the fluid that surrounds the tube. The theoretical analysis presented by Hsu et al. showed that this new measuring concept is feasible and the previously mentioned shortcomings of the conventional internal flow based measuring system can be prevented. This paper reports the result of an experimental verification of the previous theoretical analysis presented by Hsu et al (2008). A nearly simply supported slender thin aluminum tube was manufactured and tested while it was immersed in a fluid filled tank. The experimental results agree reasonably well with the theoretical results. The previous theoretical claim on the feasibility of using the external fluid loading on a vibrating tube for the measurement of fluid density is substantiated.

Similarly to the external fluid mass loading of the tube (Hsu, Hwang, and Huang., 2008), the variation of resonance frequency of the thin plate in vacuum and which immersed in the water or suspended sediment concentration (SSC) in river will be presented in this paper. For the theoretical deviation of thin plate with fluid loading, several exact and numerical methods have been developed from elasticity theory and corresponding to the boundary condition of fluid structural interactions. (Auld and Solie, 1973; Skelton and James, 1992, 1997; Rokhlin and Wang, 2002; Chen et al., 2007). In addition to the discussion of the effect of the mass loading or acoustic radiation loss by the fluid medium, the changes of the resonance frequency with the mode number and various specific gravity are also discussed by using

analytical numerical calculation and the finite element simulation. Finally, based on the theoretical analysis, the size analysis including the  $L_x$ ,  $L_y$ , and thickness ( $h$ ) of thin plate for the relation between square resonance frequency and specific gravity using in the onsite measurement are proposed.

## 2 Basic equation of a rectangular plate

Consider a rectangular plate with length  $2L_x$  and width  $2L_y$  subjected to lateral point load  $f_z(x, y, t)$  and fluid pressures  $p_t(x, y, t)$  and  $p_b(x, y, t)$  on the upper and lower surface of the plate as shown in the Fig. 1. If the plate is simply supported on the edges, boundary conditions require that the transverse displacement  $w(x, y)$  and its second derivatives vanish at the plate ends. That is,

$$\begin{aligned} (x, y) = 0, \quad \frac{\partial^2 w}{\partial y^2} = 0 \quad \text{at } x = -L_x, L_x \\ w(x, y) = 0, \quad \frac{\partial^2 w}{\partial x^2} = 0 \quad \text{at } y = -L_y, L_y \end{aligned} \quad (1)$$

The equation of bending motion for an orthotropic thin plate is given by (Leissa, 1993; Skelton and James, 1997).

$$D_{11} \frac{\partial^4 w}{\partial x_1^4} + 2H \frac{\partial^4 w}{\partial x_1^2 \partial x_2^2} + D_{22} \frac{\partial^4 w}{\partial x_2^4} + \rho_s h \frac{\partial^2 w}{\partial t^2} = f_z(x, y, t) - p_t(x, y, t) + p_b(x, y, t) \quad (2)$$

where  $\rho_s$  and  $h$  are the density and thickness of the thin plate;  $H = D_{12} + 2D_{66}$  is termed as the effective torsion rigidity of the plate, and  $D_{12} = \nu_1 D_{22} = \nu_2 D_{11}$ .

To satisfy the equation of motion and the simply supported boundary conditions, the following displacement function is introduced:

$$w(x, y, t) = \sum_{m=1}^{\infty} \sum_{n=1}^{\infty} W_{mn} \cdot [\sin k_m(x + L_x) \sin k_n(y + L_y) \cdot e^{-i\omega_{mn}t}] \quad (3)$$

where  $W_{mn}$  is the corresponding Fourier coefficients of  $w(x, y)$ ,  $k_m = (m\pi/2L_x)$  and  $k_n = (n\pi/2L_y)$ .

Substituting equation (3) into (2) and setting  $f_z = 0$  results in the following characteristic equation:

$$W_{mn} \cdot [D_{11}k_m^4 + 2Hk_m^2k_n^2 + D_{22}k_n^4 - \rho_p h \omega_{mn}^2 + f_\ell] = 0 \quad (4)$$

where  $f_l$  is the fluid pressure loading per unit transverse displacement,  $W_{mn}$ , imposed on the plate surface and the corresponding equation can be represented as

$$f_\ell(m,n) = \frac{-i\rho_t\omega^2}{\sqrt{(\omega/c_t)^2 - k_x^2 - k_y^2}} - \frac{i\rho_b\omega^2}{\sqrt{(\omega/c_b)^2 - k_x^2 - k_y^2}} \quad (5)$$

It can be obtained through the linearized Euler equation which relates pressure to the transverse displacement distributed in the plate. Here,  $k_x$  and  $k_y$  are propagation wavenumbers along  $x$  and  $y$  directions, respectively. The fluid loading terms act as a radiation damping for acoustic wavenumbers  $[(\omega/c_i)^2 > (k_x)^2 + (k_y)^2]$ , and as a added mass for  $[(\omega/c_i)^2 < (k_x)^2 + (k_y)^2]$ , where  $c_i$  is set to  $c_t$  and  $c_b$  for upper and lower halfspaces, respectively.

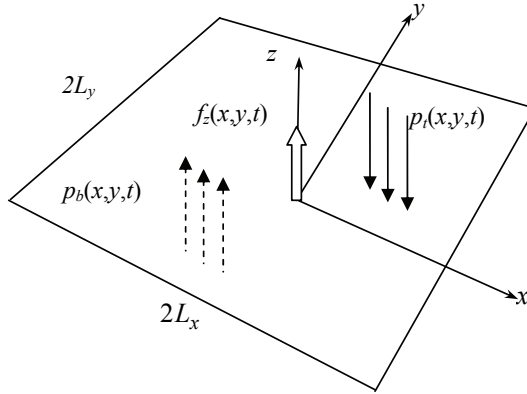


Figure 1: The schematic geometry of the rectangular plate.

### 3 Fluid loading discussions

Equation (5) shows that fluid loadings may provide added masses to a plate. It also points out that, for a given fluid medium, the loading depends on the exciting angular frequency ( $\omega$ ), wavenumber ( $k_i$ ), and the dimensions ( $L_x$  and  $L_y$ ) of the plate. Obviously, it is remarked that the fluid loading is proportional to the fluid density ( $\rho_i$ ). We may choose to compare the relative magnitudes of fluid loadings of a wave train at a particular wavenumber ( $k_{mx}, k_{ny}$ ), especially in the wavenumber of the first three simply supported bending mode ( $m=1, 2, 3; n=1$ ). The fluid loading at any angular frequency is caused by the plate vibratory response to an external excitation at that frequency. The example given here is an aluminum ( $E=7.5 \times 10^{10}$

Pa,  $\rho_s=2700 \text{ kg/m}^3$ ,  $\nu=0.3$ ) rectangular plate with  $h=3 \text{ mm}$ ,  $L_x=30 \text{ cm}$ , and  $L_y=15 \text{ cm}$ . Both the upper and lower fluids are pure water ( $\rho_w=1000 \text{ kg/m}^3$ ,  $c_w=1500 \text{ m/s}$ ). Using the aluminum plate, the comparisons between the first three fluid loadings normalized by  $(\rho_f c_f \omega)$  are shown as Fig. 2 and Fig. 3 for lower and higher frequencies, individually.

The Fig. 2 shows that the external fluid loading acts as mass loadings and without any acoustic radiation loss below 2500 Hz due to only negative real parts of the fluid loadings in the plate. In addition, the fluid mass loading of the lower mode,  $(m,n)=(1,1)$ , will increase faster than other higher mode obviously. It is meaning that, in the low frequencies, the mass loading caused by fluid medium is almost contributed from the fundamental mode.

With the increment of frequencies, shown in the Fig. 3, the mass loading by external fluid grows exponentially and reaches its maximum value when the frequency is approaching to 2795 Hz, where the wavenumber of the surrounding fluid loading is equal to the plate ( $\omega/c_f$ ). When frequencies exceed 2795 Hz, this effect of mass like loading from external fluid in the mode (1,1) abruptly turns into the acoustic radiation loss and radiates to the external medium due to the vanish of the real parts and replace to the imaginary parts. The similar variations of the fluid loading type can also be obtained for each higher mode number, especially at their corresponding critical frequency, 3535 Hz for (2,1) mode and 4507 Hz for (3,1) mode. After these critical frequencies of each mode, the acoustic radiation loss will decrease rapidly and converge asymptotically to a constant value in the further higher frequency. It is considerably discrepancy with the cylindrical thin shell because of the existence of both mass like and radiation loss in the higher frequencies for the specific mode.

## 4 Effects of resonance frequencies of a simply supported plate with fluid loading

### 4.1 Variations of resonance frequencies with fluid loading

Once the fluid loading is determined, the resonance frequencies of the simply supported thin plate considering the fluid loading can be determined from equation (4). It is remarked that the fluid loading term  $f_l$  is frequency dependent. To find resonance frequencies of the plate, it is therefore necessary to calculate the unloaded ( $f_l=0$ ) resonance frequency first, and then use this resonance frequency as the frequency parameter for estimating  $f_l$  in equation (4). The estimated  $f_l$  is then substituted into equation (4) to calculate the first fluid loaded frequency, which will be used again for calculating the new  $f_l$ . Subsequently, the second resonance frequency is calculated by using the new  $f_l$ . The iteration process will be repeated

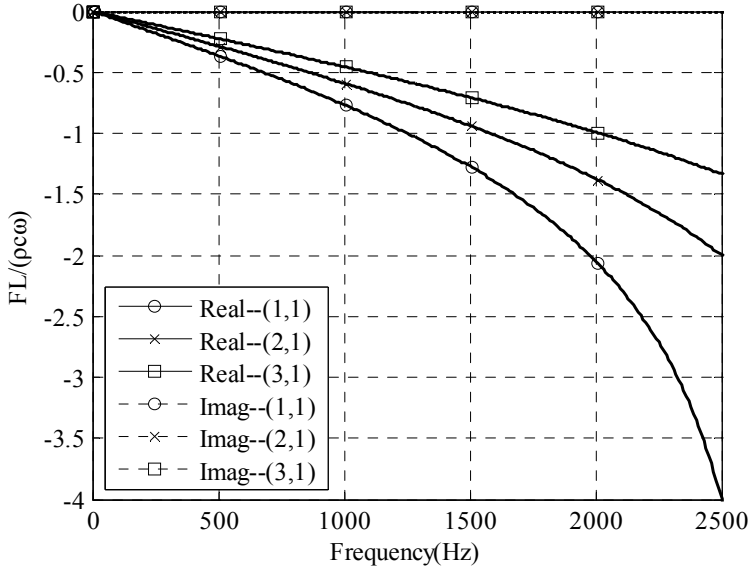


Figure 2: Fluid loading by pure water on the aluminum rectangular plate normalized by  $(\rho c \omega)$  for  $n=1$  and  $m=1, 2,$  and  $3$  from frequency  $0$  to  $2500\text{Hz}$ .

continuously until the calculated frequencies converge to a constant value.

Here again, we use the aluminum rectangular thin plate, where  $h=0.03$  cm and  $2L_x=30$  cm and  $2L_y=15$ cm, as an example. In the beginning, assuming this thin plate is in vacuum and then immersed in pure ware completely. The convergence of numerical calculated resonance frequency with  $(m,n)$  is shown in Tab. 1.

Table 1: Convergence of the iterations for the resonance frequency (kHz) of aluminum thin plate with  $(m,n)$ .

$(m,n)$		<i>In vacuum</i>	<i>In Water</i>		
			<i>Iteration -1</i>	<i>Iteration -2</i>	<i>Iteration -3</i>
$m=1$	$n=1$	417.548	122.733	122.876	122.876
	$n=2$	668.078	218.208	218.598	218.598
	$n=3$	1085.624	394.123	395.210	395.210
	$n=4$	1670.191	663.729	666.392	666.388
$n=1$	$m=1$	417.548	122.733	122.876	122.876
	$m=2$	1419.662	545.473	547.376	547.373
	$m=3$	3089.853	1387.543	1396.920	1396.889
	$m=4$	5428.120	2701.677	2730.773	2730.571

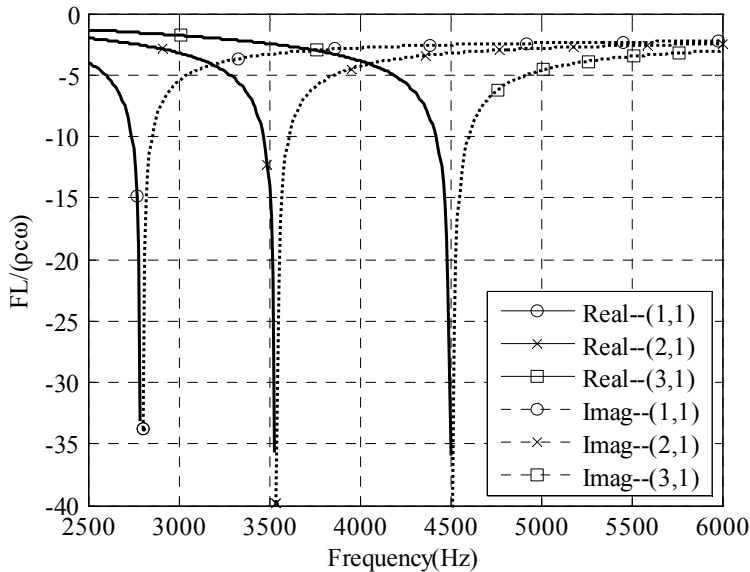


Figure 3: Fluid loading by pure water on the aluminum rectangular plate normalized by  $(\rho c \omega)$  for  $n=1$  and  $m=1, 2,$  and  $3$  from frequency 2500 to 6000Hz.

In most case, even for the higher mode  $(m,n)$ , the resonance frequency with fluid loading will converge to a constant value after only two or three calculating iterations. On the other hands, it also shows that the first resonance frequency with external fluid loading in the thin plate will reduce to almost one-third of its in vacuum. This ratio will slightly decrease with the increment of mode number  $(m,n)$ , but these ratios will maintain almost twic to third time in the more higher modes.

The comparisons of the resonance frequencies, among the unloaded (in vacuum) and loaded the plate are depicted in Fig. 4. It is shown that the fluid loading by pure water have significantly changed the thin plate's resonance frequencies from its in the vacuum values. This difference between in vacuum and in water increases apparently with the mode number  $(m,n)$ . In other words, the external fluid loading will suppress the increment of the resonance frequencies in the lower modes number than these in the higher mode numbers.

#### 4.2 Variations of resonance frequencies by SSC

Since the increase in mass density or corresponding specific gravity of water in rivers is correlated with the various suspended sediment concentration (SSC), the variations of resonance frequencies of thin plate due to the change in the specific



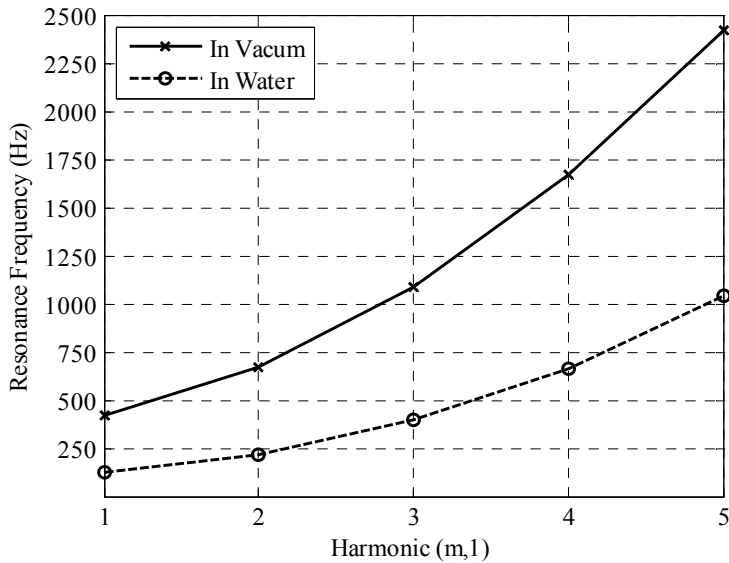


Figure 4: The resonance frequencies of bending vibrations of the thin plate for  $n=1$  and  $m=1\sim 5$  modes in the vacuum and corresponding frequencies with fluid loading by using numerical approach.

gravity of the external fluid loading should be investigated. In order to validate the influence of resonance frequencies in specific gravity of external fluid, the analytical results will not only be calculated by the numerical approach represented above, but also simulated by the finite element software, COMSOL. Similar to the previous example for aluminum thin plate, the influence of resonance frequencies in various specific gravity which varied from 1.0 to 1.5 is discussed and shown the results in the Fig. 5. As expected, since the impact of external fluid as an added mass to the thin plate, the resonance frequencies apparently shifted to the lower frequencies when the fluid specific gravity increased. On the other hand, the accuracy by using theoretical numerical analysis is demonstrated from the COMSOL finite element simulation because of the same variation with the numerical result for diverse specific gravities shown in the same figure.

The difference ratio of resonance frequency for each specific gravity calculated by numerical approach and COMSOL finite element simulation are shown in the Fig. 6. This result shows that the difference ratios are almost the same for each mode even the specific gravity increase and this difference ratio will decrease apparently with the mode. In other words, the resonance frequency of the thin plate with fluid loading evaluated by theoretical numerical approach is reasonable and properly

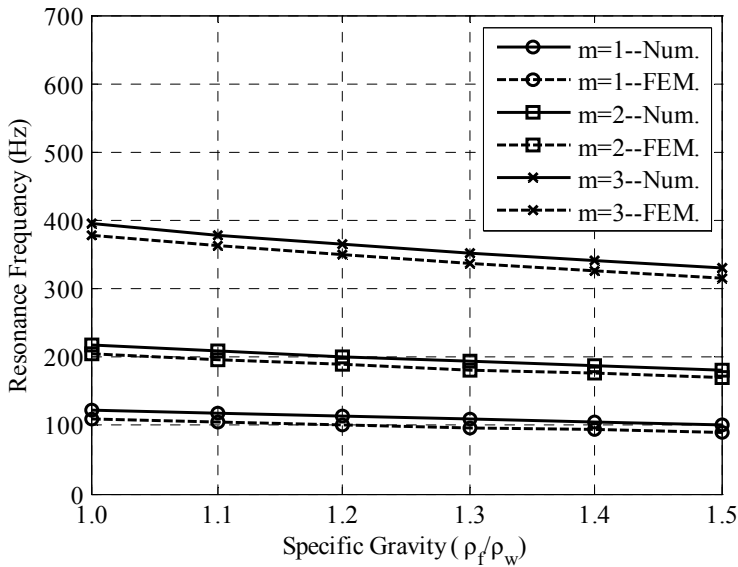


Figure 5: The relations between resonance frequencies and the specific gravity of fluid loading on the thin plate for  $n=1$  and  $m=1\sim 3$  by numerical calculation and COMSOL FEM simulation.

enough. Based on this result, it is reasonable for the simulation of the complicated model by using the COMSOL finite element.

#### 4.3 Useful approach to estimate the undetermined specific gravity of the fluid

A useful approach to estimate the undetermined specific gravity of the fluid on the vibrating plate is to use the relationship between the specific gravity ratio ( $\rho_0/\rho_w$ ) and the square of the resonance frequency ratio ( $\omega_w/\omega_0$ )<sup>2</sup>. Fig. 7 shows these relations from (1,1) to (3,3). In these modes, the increases in the squares of the frequency ratios are almost directly proportional to the increase in the specific gravity. The lower the mode number is, the larger the slope between specific ratio and square of resonance frequency will be. These slopes for mode number (1,1) to (3,3) can be calculated to vary from 0.92~0.78. In practice, the slope of the fundamental mode number of thin plate is most important than others because of the visualization of the first mode for measurement. Therefore, the formulation applied to estimate the undetermined specific gravity of the fluid can be obtained as bellow

$$(m, n) = (1, 1), \quad \frac{\rho_0}{\rho_w}; \quad 1 + 1.09 \left( \frac{\omega_w^2}{\omega_0^2} - 1 \right) \quad (6)$$

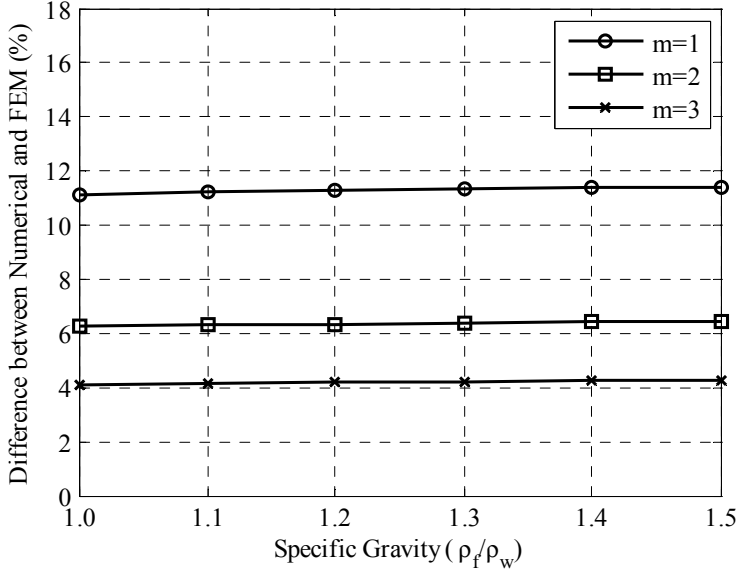


Figure 6: The difference ratio of resonance frequency with fluid loading calculated by numerical calculation and COMSOL FEM simulation for specific gravity for  $n=1$  and  $m=1\sim 3$ .

For the application, when the resonance frequency of a thin plate discussed above immersed in a river water can be measured, the mass density of the river water can be calculated from equation (6).

#### 4.4 Analysis of size effect for the rectangular plate with fluid loading

In order to realize the influence of square of frequency ratio  $(\omega_w/\omega_0)^2$  in the dimensional directions of the rectangular plate, the variations with lengths ( $L_x, L_y$ ) and thickness ( $h$ ) for mode number (1,1) and (3,3) are discussed and shown as Fig. 9 and 10, respectively. Fig. 8 shown that there is slight influence in the square of the resonance frequency ratio  $(\omega_w/\omega_0)^2$  in the fundamental mode (1,1) and higher mode number (3,3) even the length of  $y$ -direction is four time of  $x$ -direction. In other words, the variations of slope between the specific gravity and square of resonance frequency are rarely affected by the dimension of thin plate.

For the effect of thickness ( $h$ ) of thin plate, shown in the Fig. 9, the slope decreased apparently with the thickness. This is because that the increment of thickness of thin plate mainly increases the plate mass and corresponding inertia force. In other

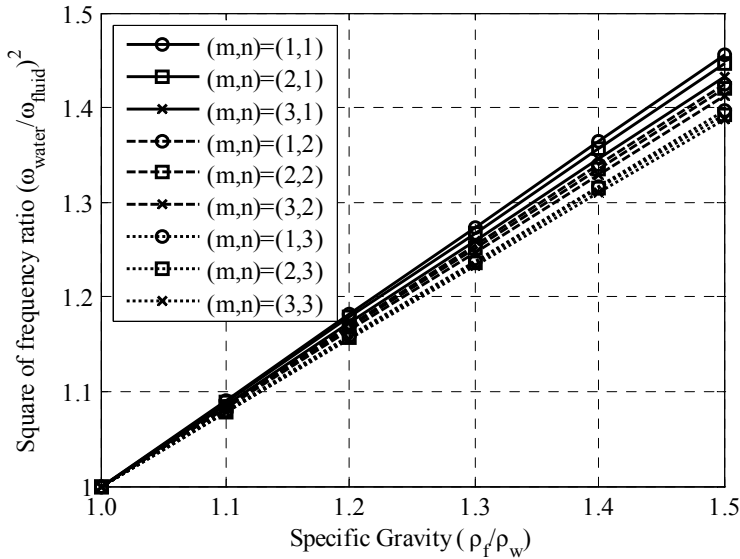


Figure 7: The relations of the square of resonance frequencies ratio  $(\omega_w/\omega_0)^2$  related to the specific gravity of fluid on the thin plate with  $(m,n)$ .

words, it will decrease the resonance frequency of thin plate. For the thin plate, thickness is equal to 0.5 mm, the slope of the mode (1,1) is approximately the same with the mode (3,3). The difference between mode (1,1) and (3,3) will increase with the thickness apparently. Therefore, before the application of thin plate for on-site measurement, the coefficient of the slope in the equation (6) must be re-simulated and modified in the laboratory according desired dimension of the plate, especially in the thickness of plate.

#### 4.5 A preliminary experiment for the demonstration of the feasibility

In order to verify the feasibility of the proposed concept, an experimental prototype for the thin plate shown in Fig. 10 can be obtained. In the convenience of the production, the clamped boundary condition of this prototype may be used. However, in the numerical analysis, it is difficult to find the adequate shape functions for the clamped boundary condition. Therefore, the COMSOL finite element simulation will be used to compare with the final experimental results. The various concentrations of the fluid can be mixed by the pure water and sodium metasilicate ( $\text{Na}_2\text{O} \cdot \text{SiO}_2$ ). To make sure the uniformly distribution of the fluid concentration in the finite space, the stirring rod in the process is necessary. The signal adaptor

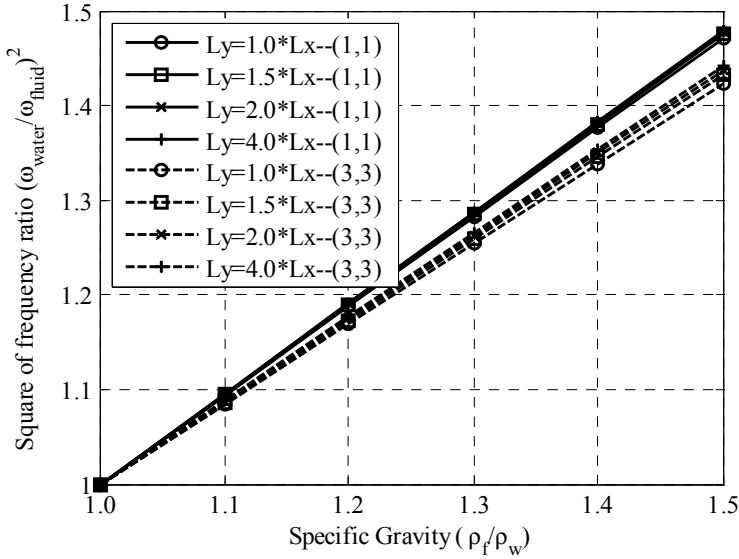


Figure 8: The relations of the square of resonance frequencies ratio  $(\omega_w/\omega_0)^2$  related to the specific gravity of fluid on the thin plate with  $(m,n)=(1,1)$  and  $(3,3)$  for a variety of  $(L_y/L_x)$ .

(IMC CRONOS-PL2) can be used to pick up the output signal and transfer by FFT. Fig.11 shows the comparison of the first four resonance frequency in the specific gravity range from 1.0 to 1.5. As shown in the figure, the fundamental mode frequencies are virtually the same whether the specific gravity is increased to 1.5. The similar results can also be found in other higher modes. These results show a similar trend on the calculated effects by the external fluid loading shown in Fig. 5. The difference between Fig. 5 and Fig.11 is the boundary condition and the geometric scale. Therefore, although this is a rather crude experiment, the result is believed adequate to demonstrate the feasibility of the concept.

## 5 Conclusions

An investigation of using the external fluid loading on the vibrating rectangular thin plate has been presented. The fluid loading, like the added mass loading, by the external fluid on the vibrating thin plate has been evaluated analytically. The accuracy of the resonance frequencies with specific gravity by using the numerical approach presented in this paper is demonstrated from the finite element simulation, COMSOL. The rapid processes and explicit results is the advantage of using the nu-

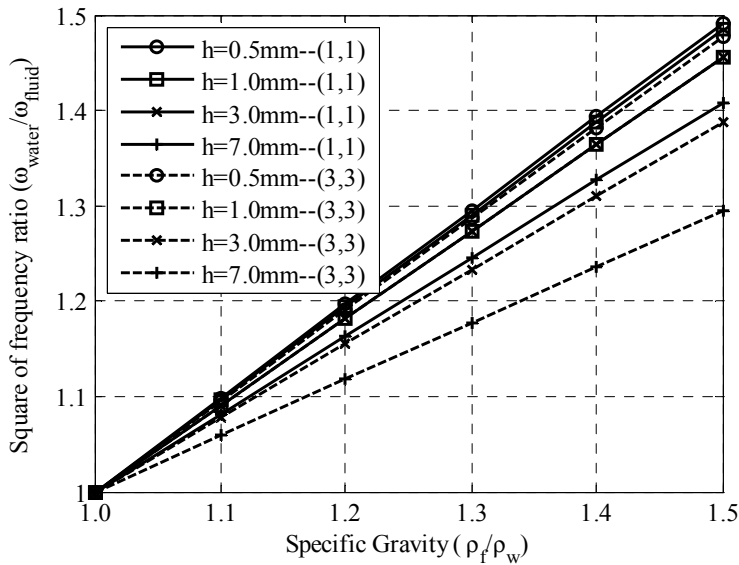


Figure 9: The relations of the square of resonance frequencies ratio  $(\omega_w/\omega_0)^2$  related to the specific gravity of fluid on the thin plate with  $(m,n)=(1,1)$ ,  $(3,3)$ , and  $(L_xL_y)=(15\text{ cm},7.5\text{ cm})$  for a variety of the thickness  $(h)$  of plate.

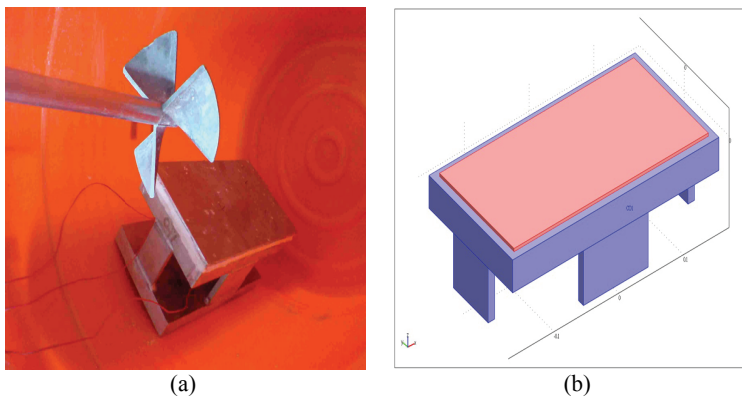


Figure 10: The prototype of the thin plate; (a) experimental model; (b) simulated model.

merical approach. The result shows that resonance frequencies change are sensitive enough to have the possible resolution on the various fluid specific gravity to the pure water. The relationships between the square of the resonance frequency ratio

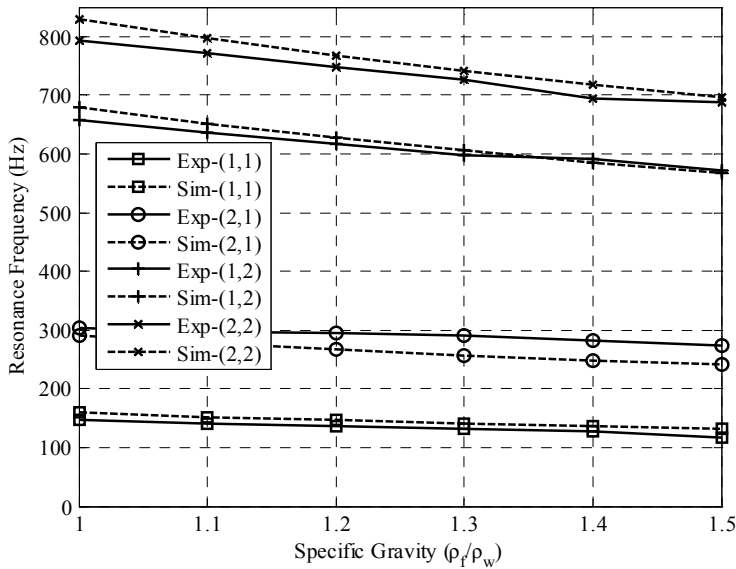


Figure 11: The comparisons between experiment and simulation for first four modes.

and specific gravity related to the pure water are discussed in this paper. The variation of these coefficients for the estimated formulation related to the dimensions in  $x$ -,  $y$ -, and  $h$  directions are also presented and discussed. It is very convenient and rapid to be referred to the design of the thin plate in advance and be used to estimate the unknown specific gravity of fluid in the onsite measurement. Finally, the preliminary experiment of the plate immersed in the fluid loading with various specific gravity are also accomplished. The comparison shows the good agreement with the experiment and finite element simulation. Therefore, based on the results of the theoretical analysis and the experiment shown in this paper, the concepts using the loading by the external fluid on the vibrating thin plate is feasible.

## References

- Auld, B. A.; Solie, L. P.** (1973): Elastic waves in free anisotropic plates. *J. Acoust. Soc. Am.*, vol.54, no.1, pp. 50–65.
- Chen, W.Q.; Wang, H. M.; Bao, R.H.** (2007): On calculating dispersion curves of waves in a functionally graded elastic plate. *Compos. Struct.*, vol. 81, no. 2, pp. 233–242.
- Guy, H.; Norman, V.** (1970): *Field Methods for Measurement of Fluvial Sediment.*

U. S. Geological Survey, Chapter C2, Book 3.

**Henry, M.** (2000): Self-validating Digital Coriolis Mass Flow Meter. *Comput. Control Eng.*, vol. 11, no. 5, pp.219–227.

**Hinghofer-Szalkay, H.** (1986): Method of high precision micro sample blood and plasma mass densitometry. *J. Appl. Physiol.*, vol. 60, no. 3, pp. 1082–1088.

**Hsu, Y. S.; Cai, J. F.** (2010): Densimetric Monitoring Technique for Suspended Sediment Concentrations. *J. Hydraul. Eng.-ASCE*, vol. 136, no. 1, pp. 67–73.

**Kalotay, P.** (1999): Density and Viscosity Monitoring Systems using Coriolis Flow Meters. *ISA Transaction*, vol. 38, pp. 303–310.

**Leissa, W.** (1993): *Vibration of Plates*. Acoustical Society of America, New York.

**Rogerson, G. A.; Kossovitch, L.Y.** (1999): Approximations of the dispersion relation for an elastic plate composed of strongly anisotropic elastic material. *J. Sound Vib.*, vol. 225, no. 2, pp. 283–305.

**Sultan, G.; Hemp, J.** (1989): Modelling of the Coriolis Mass Flowmeter. *J. Sound Vib.*, vol. 132, no. 3, pp. 473–489.

**Skelton, E. A.; James, J. H.** (1992): Acoustics of anisotropic planar layered media. *J. Sound Vib.*, vol. 152, no. 1, pp. 157–174.

**Skelton, E. A.; James, J. H.** (1997): *Theoretical acoustics of underwater structures*. World Scientific Publishing Company, London.

**Hsu, Y. S.; Hwang, Y. F.; Huang, J. H.** (2008): An exploratory study of using external fluid loading on a vibrating tube for measurement suspended sediment concentration in water. *J. Phys. D: Appl. Phys.*, vol. 41, no. 16, pp. 165504–165513.